Journal of Operation and Automation in Power Engineering
Vol. 4, No. 1, Winter & Spring 2016, Pages: 66-82
http://joape.uma.ac.ir

Control of Inverter-Interfaced Distributed Generation Units for Voltage and Current Harmonics Compensation in Grid-Connected Microgrids

R. Ghanizadeh[1], M. Ebadian[1,*], G. B. Gharehpetian [2]

[1]Department of Electrical and Computer Engineering, University of Birjand, Birjand, Iran.
[2]Department of Electrical Engineering, Amirkabir University of Technology, Tehran, Iran.

ABSTRACT

In this paper, a new approach is proposed for voltage and current harmonics compensation in grid-connected microgrids (MGs). If sensitive loads are connected to the point of common coupling (PCC), compensation is carried out in order to reduce PCC voltage harmonics. In absence of sensitive loads at PCC, current harmonics compensation scenario is selected in order to avoid excessive injection of harmonics by the main grid. In both scenarios, compensation is performed by the interface converters of distributed generation (DG) units. Also, to decrease the asymmetry among phase impedances of MG, a novel structure is proposed to generate virtual impedance. At fundamental frequency, the proposed structure for the virtual impedance improves the control of the fundamental component of power, and at harmonic frequencies, it acts to adaptively improve nonlinear load sharing among DG units. In the structures of the proposed harmonics compensator and the proposed virtual impedance, a self-tuning filter (STF) is used for separating the fundamental component from the harmonic components. This STF decreases the number of phase locked loops (PLLs). Simulation results in MATLAB/SIMULINK environment show the efficiency of the proposed approach in improving load sharing and decreasing voltage and current harmonics.

KEYWORDS: Distributed generation, Microgrid, load sharing, Voltage and current harmonics compensation, Self-tuning filter.

1. INTRODUCTION

A microgrid (MG) is a controllable network which includes distributed generation (DG) units, energy storage systems, and distributed loads. An MG can be utilized in two modes; grid-connected mode and independent (islanded) mode [1-2]. Optimal utilization of MGs removes the need for building new transmission networks, decreases environmental pollution, reduces energy losses in transmission and distribution networks, increases power quality, and creates new approaches for using renewable energy resources [2-4]. Also, the great increase in using nonlinear loads at distribution voltage levels, has changed the voltage and current harmonics into a common problem for the power quality of MGs. These problems might have undesirable effects such as interruption in the operation of adjustable speed drives (ASDs) and protective relays, motors and transformers overheating, and errors of power factor correction capacitors [5].

DGs are usually connected to electrical systems through a power electronic converter. The main role of an interface converter is to control the active and reactive powers injected by the DG. In addition, using appropriate control approaches, these converters can also be used to compensate for power quality problems. The control system of each DG includes controllers of fundamental component of the power, controllers of current, voltage, and virtual impedance loop. The characteristics used for

Received: 4 Sep. 2015 Revised: 8 Nov. 2015
Accepted: 29 Jan. 2016
*Corresponding author:
M. Ebadian (E-mail: mebadian@birjand.ac.ir)

controlling the fundamental components of powers, are only capable of sharing the positive sequence of the fundamental component of the load current among DGs. But other components of the load current such as harmonic components, are shared based on the impedances between each DG and the position in which the load is installed (including the impedance of DG and line impedance). Therefore, in previous studies, some methods have been presented to improve the sharing of nonlinear loads among the interface converters of DGs.

A method was presented in Ref. [6] for improving the sharing of distortion power (*D*) among DGs. In this approach, *D* is shared by adjusting the voltage control bandwidth, which is done since the voltage control gain increases as *D* increases and causes the nonlinear load sharing to be improved. However, this approach has a disadvantage; it decreases voltage control stability [7]. In Refs. [7-11], some methods have been presented for sharing nonlinear load among DGs, which are based on creating a virtual impedance on the path of currents of harmonic components. In Ref. [8], a control strategy was proposed for sharing harmonic power in an islanded MG. The proposed control strategy employed negative virtual harmonic impedance to compensate for the effect of line impedance on harmonic power delivery. In Ref. [7], the harmonic current of any order was proposed to be used for creating a voltage drop which could lead the current by 90 degrees. By doing so, a virtual inductance can be created at harmonic frequencies. However, a virtual resistance is usually preferred to a virtual inductance since its impedance value does not depend on frequency and on the other hand, it helps damp the system oscillations; however, inductance will have a large impedance value at high frequencies, disturbing the output voltage of DGs. In this regard, in Ref. [11], fixed harmonic resistances were used.

Using fixed values for virtual impedance which has been proposed in Refs. [7-11] cannot lead to a proper nonlinear load sharing in MGs which are remarkably asymmetric from the load distribution or lines impedance points of view.

In this paper, a structure is proposed for the virtual impedance, to adaptively improve the nonlinear load sharing among DGs at harmonic frequencies. In the proposed structure, virtual resistances with variable values is used for different harmonic frequencies. The value of harmonic resistance of each DG is determined based on the amount of the nonlinear load supplied by it. Therefore, the effect of the asymmetry of MG impedances is significantly decreased. However, it must be noted that a proper nonlinear load sharing among DGs causes distortion in DG outputs and consequently increases PCC harmonics.

So far, several approaches have been presented for controlling MGs, which aim to compensate for voltage and current harmonics. In general, these approaches either are based on autonomous control of the interface converter of DG or use a central controller to compensate for distortions. In this regard, in Ref. [12], a single phase DG was considered which acted as a shunt active filter. In other words, DG injected harmonic currents to improve the voltage quality. In Refs. [13-14], an optimal control approach based on particle swarm optimization (PSO) algorithm has been used to improve the power quality parameters. In this approach, PSO is responsible for optimally adjusting the control parameters of the system in order to satisfy the power quality requirements especially adjusting voltage and frequency. In Ref. [11], a control approach based on the selective compensation of voltage harmonics was presented for an MG, which was connected to the main grid. In Refs. [15-18], several approaches have been proposed for the local control of DGs, in which the idea of resistive behavior has been used to compensate for voltage harmonics. The authors of [17] presented a local control technique for islanded MGs. In their solution, in addition to power controllers and inner control loops of voltage and current, a load compensator was used. In this compensator, a fundamental component virtual impedance loop was used for improving the droop performance of the controllers and a harmonic virtual impedance loop was used for sharing nonlinear load among DGs. In Ref. [18], droop characteristics based on harmonic reactive power were been used to share the compensation workload among DGs. In this regard, the authors of [19]

proposed an approach to share the compensation workload of DGs using the free capacity of the interface converters. In Ref. [20], a control approach was presented for coordinating the interface inverters of DGs and the active power filters for the compensation of voltage harmonics in MGs. Simulation results showed that coordinated control is an approach which can be useful in spite of limitation in the rated power of the interface converters or too much distortion at the output voltages of DGs due to participation in the compensation for power quality problems. In Ref. [21], a control algorithm was proposed to compensate for voltage and current harmonics. The proposed compensation system can be operated in both grid-connected and islanded operations of the MG system without changing any configuration.

In most of the aforementioned methods, voltage harmonics compensation has been carried out at DG output bus. However, the power quality at PCC is of great importance because some sensitive loads which require high power quality, might be connected to it. Furthermore, when DGs try to locally compensate for voltage harmonics at their own output bus or a bus nearby, harmonic distortion might increase at some other buses of the electrical system (such as the sensitive load bus). Therefore, by directly compensating for the PCC voltage harmonics, proper power quality is guaranteed for sensitive loads. Moreover, compensation for the voltage harmonics of PCC causes the mutual effect of power quality distortion at MG and the main grid to decrease [11, 22]. On the other hand, if sensitive loads do not exist at PCC and the mutual effects of grid disturbances are insignificant, current harmonics compensation scenario which is aimed to prevent the main grid from injecting too much harmonic currents is more important. Using current harmonics compensation scenario decreases the thermal tension created in the grid connection transformer caused by the flow of harmonic currents also, it prevents the voltage disturbances of the adjacent buses of PCC in the main grid caused by the flow of harmonic currents [5, 11].

In this paper, a new approach is presented for the local control of DGs, which is aimed to compensate for PCC voltage or main grid current harmonics. This compensator is capable of adjusting compensation percentage in proportion with the existing level of disturbance at PCC or main grid. Also, this controller provides a proper sharing of compensation workload, considering the nominal capacity of DGs, which will improve the nonlinear load sharing. In the structures of the proposed harmonic compensator and virtual impedance blocks, a self-tuning filter is used to separate the harmonic component from the fundamental components. This issue results in the reduction of the number of the phase locked loops (PLLs).

2. CONTROL SYSTEM OF DGS OF MG

Fig. 1 shows the single line diagram of a grid-connected MG which includes several DGs with power electronic interface converter and some balanced linear and nonlinear loads. The MG is connected to the main grid through a distribution line with the impedance of Z_g, and a transformer with the equivalent impedance of Z_t. As can be seen, the harmonic voltage at PCC, ($V_{PCC,abc}$), and the main grid current harmonic ($i_{g,abc}$) are extracted by measurement blocks and sent to all the local controllers of DGs. Considering the fact that there may be a large distance between PCC and DGs, a low-bandwidth communication (LBC) is used for transmitting harmonics data. The selection of the LBC is aimed to avoid the dependency of the operation of the control system on the existence of a high bandwidth (which can decrease system reliability). It is assumed that data transmission through LBC has a delay of 1 ms. On the other hand, in order to make a low bandwidth sufficient for transmission, the data to be transmitted by the LBC must include nearly dc signals [11, 20, 22]. Thus, in this paper, first the voltage harmonic components of the PCC or current harmonic components of the main grid in synchronous reference frame (dq) are extracted and sent to local DG controllers.

The details of the scheme proposed for control system of DGk together with its power stage are shown in Fig. 2. As can be seen in this figure, the voltage and current harmonics are compensated at the local control level. The power stage of each DG is composed of a dc link, an interface converter of voltage source type, and an LC filter. Since the

approach proposed in this paper is focused on controlling DG interface converters, it is assumed in the simulations that a nearly constant voltage is always supplied at the dc link by the converter. As can be seen in Fig. 2, the potential fluctuation of the dc link voltage is taken into account by a feed-forward loop in generating the control signals of the converter. The local DGs control system is designed in $\alpha\beta$ reference frame, and the Clarke transformation is used for transmitting variables from the *abc* frame to $\alpha\beta$ frame [23].

As is shown in the local DG_k controller block, the reference voltage of DG in the $\alpha\beta$ frame ($v^*_{\alpha\beta}$) is generated by the droop characteristics of the power control, virtual impedance loop, and harmonics compensator block. On the other hand, the instant-aneous DG output voltage (v_{abc}) is transferred to $\alpha\beta$ reference frame, and once it is compared with $v^*_{\alpha\beta}$, it creates the current control reference ($i^*_{\alpha\beta}$). Finally, the response of the current controller to the error resulted from the difference between the current of the inductor of the filter and the reference current, $i^*_{\alpha\beta}$, is returned to *abc* reference so that the reference three phase voltages are created in this system of coordination and the DG interface converter is switched based on this reference. The details of PCC voltage and main grid current measurement technique are shown in the measurement unit of Fig. 2. In this regard, $V_{PCC,abc}$ or $i_{g,abc}$ are transferred to the *dq* reference frame which rotates at the speed of ω, where, ω is the angular frequency of the system extracted by the PLL.

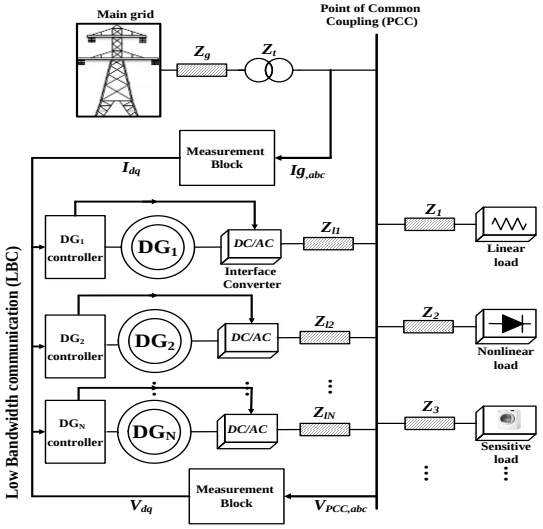

Fig. 1. Structure and control system of MG in grid-connected mode.

2.1. Controlling fundamental components of powers

In this paper, the following droop characteristics are used to share the powers of fundamental component among DGs in the grid-connected mode [7, 24].

$$\phi^* = \phi_o + (m_{pp} + \frac{m_{ip}}{s})(\bar{P}^* - \bar{P}) \quad (1)$$

$$E^* = E_o + (n_{pQ} + \frac{n_{iQ}}{s})(\bar{Q}^* - \bar{Q}) \quad (2)$$

where, $\bar{P}^*$ and $\bar{Q}^*$ are the reference active and reactive powers, $\bar{P}$ and $\bar{Q}$ are the fundamental components of the active and reactive powers, respectively, Φ_0 is the reference phase angle of the output voltage, E_0 is the reference phase voltage amplitude, m_{pp} and m_{ip} are the proportional and integral coefficients of the active power control and n_{PQ} and n_{iQ} are the proportional and integral coefficients of the reactive power control, respectively. Using droop controller for sharing power among DGs removes the need for a communicational link between local controllers. Also, these characteristics can cause a deviation in the voltage amplitude and frequency of MG. An increase in the slope of these characteristics increases the accuracy of power sharing among DGs and a decrease in their slope can decrease the deviation of DGs output voltage and frequency from their reference values. Thus, when these characteristics are used, a trade-off must be established between the accuracy of power sharing and deviation amount of voltage and frequency from their reference values.

2. 2. Inner control loops of voltage and current

Since PI controllers do not have a proper performance in controlling non-dc variables, proportional resonant (PR) controllers are preferred to be used in the $\alpha\beta$ reference frame [25]. In this paper, resonant controllers of voltage and current represented by Eqs. (3) and (4) are considered. Also, controlling the instantaneous current of the filter inductor ($I_{L\alpha\beta}$), instead of the DG output current minimizes the sensitivity of the control system to load current variations [26].

$$G_v(s) = k_{pV} + \frac{2.k_{rV}.\omega_{cV}.S}{S^2 + 2.\omega_{cV}.S + (\omega_0)^2} \quad (3)$$

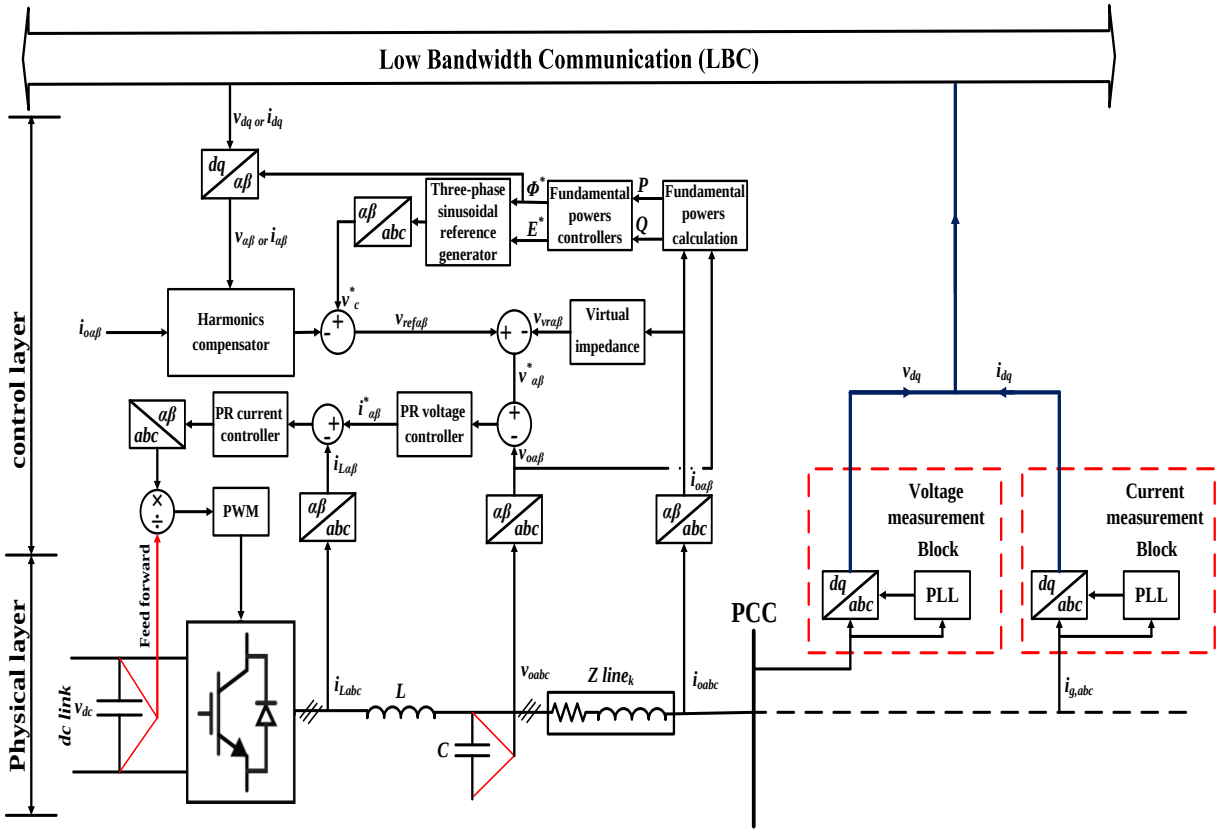

Fig. 2. Details of control system used for controlling DGk to compensate voltage or current harmonics.

$$G_I(s) = k_{pI} + \frac{2.k_{rI}.\omega_{cI}.S}{S^2 + 2.\omega_{cI}.S + (\omega_0)^2} \quad (4)$$

where, k_{pV} and k_{pI} are proportional coefficients of voltage and current controllers, respectively. Also, k_{rV} and k_{rI} are the resonant coefficients and ω_c is the cut-off frequency of the voltage and current resonant controllers.

2. 3. Self-tuning filter

In Ref. [27], Hong-Sock investigated the integral in the synchronous reference frame and showed that:

$$V_{xy}(t) = e^{j\omega t}\int e^{-j\omega t}U_{xy}(t)dt \quad (5)$$

where, U_{xy} and V_{xy} are instantaneous signals before and after integration in the synchronous reference frame. By applying Laplace transformation to Eq. (5), the transfer function of this Eq. is described as follows:

$$H(s) = \frac{V_{xy}(s)}{U_{xy}(s)} = \frac{s + j\omega}{s^2 + \omega^2} \quad (6)$$

To obtain an STF with the cut-off frequency of ω_n from the transfer function of *H(s)*, a fixed parameter, *k*, was introduced in Ref. [28], by which the transfer function of *H(s)* can be written as follows:

$$H(s) = \frac{V_{xy}(s)}{U_{xy}(s)} = k\frac{(s+k) + j\omega_n}{(s+k)^2 + \omega_n^2} \quad (7)$$

When the parameter *k* is added to *H(s)*, the amplitude of transfer function becomes limited and equal to the amplitude of the frequency component, ω_n. Furthermore, the phase delay at the cut-off frequency of ω_n is equal to zero.

By replacing the input signal $x_{\alpha\beta}(s)$ with U_{xy}, and output signal V_{xy} with $\hat{x}_{\alpha\beta}$ and also simplifying these equations, where:

$$\hat{x}_\alpha = (\frac{K}{s}[x_\alpha(s) - \hat{x}_\alpha(s)] - \frac{\omega_n}{s}\hat{x}_\beta(s) \quad (8)$$

$$\hat{x}_\beta = (\frac{K}{s}[x_\beta(s) - \hat{x}_\beta(s)] - \frac{\omega_n}{s}\hat{x}_\alpha(s) \quad (9)$$

where, ω_n is the desirable frequency at the output, and *k* is the filter gain. The accuracy of extracting the component of interest increases with the decrease in the value of *k*. Also, $x_{\alpha\beta}(s)$ and $\hat{x}_{\alpha\beta}(s)$ can be either the voltage or the current signals before and after filtering, respectively. Therefore, using an STF, the main components of distorted voltage and current signals can be obtained without delay [28-29].

Considering Eqs. (8) and (9), the block diagram of an STF is shown in Fig. 3.

The frequency response of STF versus variations of parameter k for the fundamental frequency (50Hz) is shown in Fig. 4. As can be observed, the magnitude and phase angle of the STF transfer function at fundamental frequency (50Hz) are equal to 1 and 0, respectively. Therefore, it can be said that the voltage and current references are properly tracked [29]. The STF plays a key role in the operation of harmonics compensation and virtual impedance blocks. Recently, STF has also been used in the structure of a unified power quality controller (UPQC) [29-30].

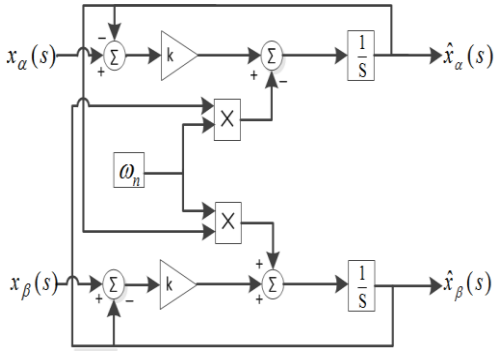

Fig. 3. Block diagram of self-tuning filter [29].

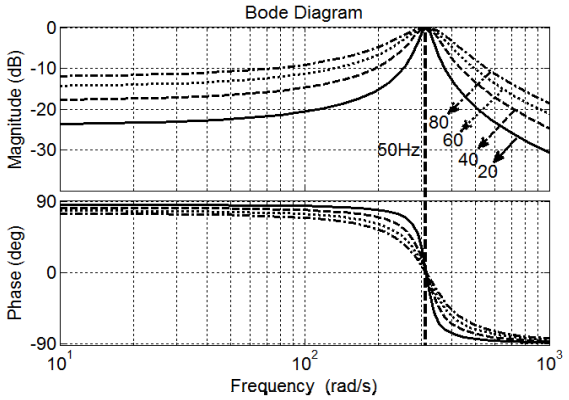

Fig. 4. Bode diagram of STF versus variations of parameter k (50 Hz) [29].

2.4. Proposed structure for virtual impedance

As mentioned, in order to control the active and reactive powers of the fundamental component, it is assumed that the system impedance is mainly inductive. Therefore, the virtual impedance is added at fundamental frequency to make the DG output impedance and consequently to make the total impedance of the system more inductive. Also, adding a virtual resistance helps damp the fluctuations in MG [7]. This damping can also be achieved using a real resistance at the cost of increasing the losses. Therefore, in order to avoid decreased efficiency, the virtual resistance which can be achieved by a lossless control loop is preferred [24] and its value must be selected such that the system impedance remains inductive.

On the other hand, in MGs, the impedance of distribution lines has a significant impact on the accuracy of power sharing among DGs. Thus, by creating virtual impedance at the fundamental frequency, the amplitude and phase of DGs output impedance can be adjusted such that the effect of the asymmetry of the line impedance on the accuracy of power sharing among DGs is minimized [31]. Fig. 5 shows the basic structure of the virtual impedance in the stationary frame, where R_v and L_v are the virtual resistance and inductance, respectively, and ω is the system frequency [31].

Also, the harmonic frequencies due to nonlinear load sharing can be improved by using a virtual impedance. Therefore, the basic structure of the virtual impedance shown in Fig. 5, is expanded by adding a virtual resistance at harmonic frequencies as shown in Fig. 6. In this figure, $R_{v,harm}$ represents the virtual resistance at harmonic frequencies. The value of $R_{v,harm}$ is adaptively determined based on the amount of the nonlinear load supplied by each DG to improve nonlinear load sharing among the DGs of MG. The non-fundamental apparent power (S_n), which can be called harmonic power, is considered as the power that is generated by each DG unit to supply the nonlinear load. According to Fig. 6, $R_{v,harm}$ is determined by Eq. (10).

$$R_{v,harm} = K_v.S_n \tag{10}$$

where, K_v is a small positive constant that is determined based on the nominal power of DGs, i.e. the greater the power of a DG, the smaller its K_v would be. S_n is calculated based on IEEE 1459-2010 standard [32] by Eq. (11).

$$S_n = S.\sqrt{(THD_I)^2 + (THD_V)^2} \tag{11}$$

where, S, THD_I, and THD_V represent the apparent power of the fundamental component, current THD and output voltage THD, respectively.

According to Eq. (11), as S_n increases, the value of $R_{v,harm}$ increases, which is a limiting factor for S_n, since the values of the resistance among DGs and the load increase at harmonic frequencies. Therefore, a virtual impedance is obtained which is composed of separate virtual impedances at fundamental and harmonics frequencies.

Extracting the harmonic and fundamental components of the DG output current is carried out based on Fig. 6. This is initially done by measuring the DG output current and then transferring it from *abc* domain to stationary reference frame ($\alpha\beta$). Then, using a self-tuning filter (STF), the fundamental and harmonic components of the DG output current are separated. Here, since balanced harmonic conditions are considered, only one of the sequences of the fundamental and harmonic components will be presented.

2. 5. Compensating for voltage or current harmonics

Fig. 7 shows the details of the harmonics compensation block of Fig. 2 for DG_k. As mentioned before, using this block, PCC voltage or the main grid current harmonics are compensated. As can be seen, the compensation reference for voltage harmonics (V^*_{hc}) is generated. Finally, the obtained value is multiplied by the ratio of the nominal power of the converter of the DG_k to the sum of nominal powers of all DGs ($\sum_{k=1}^{n} S_{0,k}$) so that the compensation reference (V^*_C) for DG_k is generated and a part of the voltage controller reference is built. By doing so, the compensation workload is shared among DGs in proportion with their nominal powers. According to Fig. 7, V^*_{hC} is generated by Eq. (12).

$$v^*_{hc} = v^h_{\alpha\beta} \text{ or } i^h_{\alpha\beta}.Gh.(THD_{I\alpha,\max} - THD_{I\alpha}) \qquad (12)$$

where, $v^h_{,\alpha\beta}$ is the PCC voltage harmonics and $i^h_{\alpha\beta}$ is the main grid current harmonics in $\alpha\beta$ reference frame. *Gh* is the gain of the harmonic compensation, which is determined based on the existing level of disturbance at PCC or the main grid. In the case of voltage harmonics compensation, considering the negative sign used for the injection of V^*_C in Fig. 7, *Gh* must be positive so that a harmonic voltage is generated in the opposite phase of $v^h_{,\alpha\beta}$ to decrease harmonic distortion at PCC.

However, to compensate for the current harmonics, a current needs to be provided by the DGs which is in the phase with the current flowing between the main grid and the MG, so that the main grid share in supplying the current of harmonic load is decreased. Therefore, *Gh* must be negative so that by considering the negative sign of the V^*_C injecion, , an in-phase compensation is provided.

In Eq. (12), $THD_{I\alpha}$ is the total harmonic distortion index of the DG output current harmonics. Fig. 7 shows how to calculate this index. As can be seen, first, the fundamental and harmonics components of the current in α axis (I^l_α and I^h_α) are extracted by the STF and, once their effective values (I^l_α and I^h_α) are calculated, they are used for calculating the $THD_{I\alpha}$. Since a balanced electrical system is considered here, using β component for calculating THD_I will provide similar results. Otherwise, under unbalanced conditions, to calculate *THD*, it is necessary to extract positive and negative sequences of harmonics, which is out of the scope of this paper. $THD_{I\alpha,max}$ is the maximum value of $THD_{I\alpha}$ which is considered to be equal to 1 here. In other words, in this system, the amplitude of the current harmonic component is always smaller than that of the fundamental component. However, a larger value can be used for $THD_{I\alpha,max}$ if necessary. In this approach, $THD_{I\alpha}$ is considered as an index for the amount of the participation of each DG in compensation so that the PCC voltage or main grid current harmonics compensation is carried out by injecting harmonic current of DGs and consequently increasing $THD_{I\alpha}$. Therefore, considering ($THD_{I\alpha,max}$-$THD_{I\alpha}$) in Eq. (12) causes the compensation workload to be shared among DGs. Because increasing workload means increasing $THD_{I\alpha}$ and as a result decreasing ($THD_{I\alpha,max}$-$THD_{I\alpha}$), it is shown that there is an intrinsic feedback in this compensation approach. The concept used for sharing compensation workload is similar to sharing powers of fundamental component among DGs of an islanded MG.

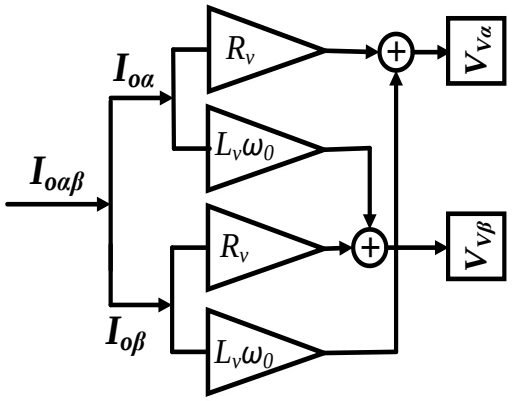

Fig. 5. Block diagram of virtual impedance [31].

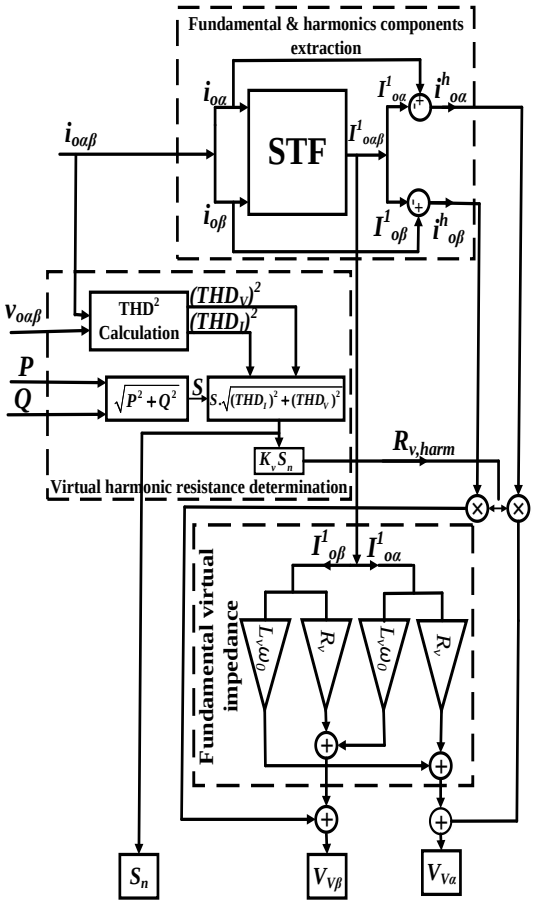

Fig. 6. Block diagram of the proposed virtual impedance.

3. DETERMINING CONTROL SYSTEM PARAMETERS

In this paper, an MG with two DGs is considered. The nominal power of DG_1 is twice that of DG_2. Therefore, the parameters of DG_1 can be determined by stability analysis and the parameters of DG_2 can be adjusted based on its nominal power. However, the stability can also be analyzed for DG_2 and similar results can be achieved. In this regard, in Ref. [11], to the manner of obtaining the droop characteristics of the power control was described.

According to Ref. [17], the local control system and the power stage of the DG can be modeled by the following Equation:

$$V_O(s) = G_{cl}(s).V_{ref}(s) - Z_O(s).I_O(s) \tag{13}$$

where, $v_{ref}(s)$, $V_o(s)$, and $I_o(s)$ are the reference voltage, and measured values of voltage and current at LC filter output, respectively, as shown in Fig. 2. Also, $G_{cl}(s)$ and $Z_0(s)$ represent the transfer function of the closed loop control system and the output impedance of the converter, respectively, modeled by Eqs. (14) and (15).

$$G_{cl}(s) = \left.\frac{V_O(s)}{V_{ref}(s)}\right|_{Io(s)=0} = \frac{G_V(s).G_d(s).G_I(s)}{LCs^2 + (r_L + G_I(s).G_d(s)).Cs + G_V(s).G_d(s).G_I(s)} \tag{14}$$

$$Z_O(s) = \left.\frac{V_O(s)}{I_O(s)}\right|_{V_{ref}(s)=0} = Z'_O(s) + Z_V(s) \tag{15}$$

where, r_L is the resistance of the inductor of the LC filter, and $G_d(s)$ represents the transfer function of the PWM unit, which is usually modeled as a very short delay. $Z_v(s)$ is the virtual impedance in the presence of the fundamental component and $Z'_o(s)$ is the converter output impedance in the absence of the virtual impedance. The converter output impedance can be determined by the following Eq.:

$$Z'_O(s) = \frac{Ls + r_L + G_I(s).G_d(s)}{LCs^2 + (r_L + G_I(s).G_d(s)).Cs + G_V(s).G_d(s).G_I(s)} \tag{16}$$

The Bode diagrams of $Z'_o(s)$ and $G_{cl}(s)$ in positive sequence are shown in Figs. 8 and 9, respectively, using the parameters presented in Table 2. It can be seen in Fig. 8 that the magnitude and phase angle of the closed loop transfer function at fundamental frequency (50Hz) are equal to 1 and 0, respectively. Therefore, it can be said that the reference voltage is properly tracked.

As mentioned, the parameters of the virtual impedance loop at fundamental frequency should be determined in a way that the MG has a mainly inductive impedance. Also, a small value of virtual resistance can help damp the system oscillations. Accordingly, the values presented in Table 2 are

considered as parameters of the proposed virtual impedance. It should be mentioned that since the nominal power of DG_2 is half of that of DG_1, its virtual impedance values must be twice of the ones in DG_1. On the other hand, it is clear that improving harmonic load sharing is obtained at the cost of increasing the distortion of the DG output voltage due to harmonic voltage drop across the virtual resistance added at harmonic frequency. Therefore, in order to select the value of K_v, a trade-off must be established between the harmonic distortion and accuracy of nonlinear load sharing. Furthermore, the nominal powers of DGs need to be considered in selecting the value of K_v.

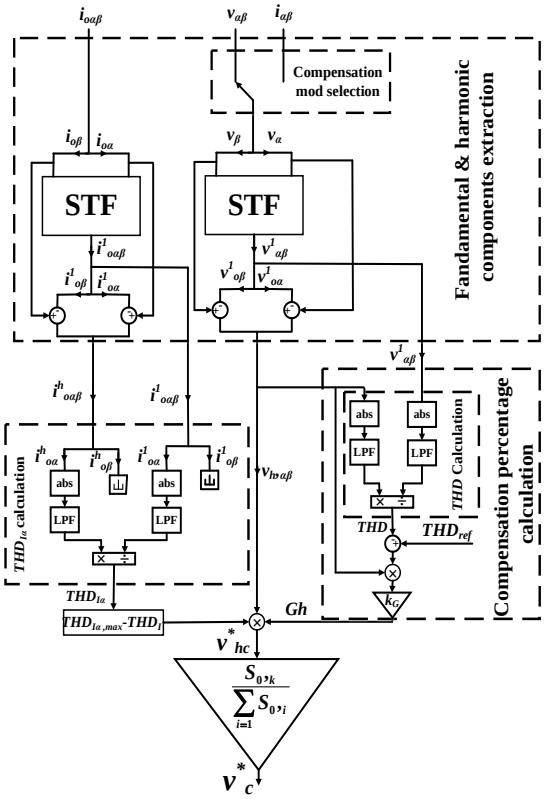

Fig. 7. Proposed harmonic compensation block for DGk.

4. SIMULATION RESULTS

The studied system is shown in Fig. 10. As mentioned before, the MG has two DGs and the nominal power of DG_1 is twice that of DG_2. The rated values of phase voltage and frequency of the MG are considered to be equal to 230V and 50 Hz. A balanced three phase load with Y connection (with the impedance of Z_L) and a full-wave three phase diode rectifier are connected to PCC as linear and nonlinear loads, respectively. It is assumed that the grid voltage has the fifth and seventh harmonics of 5% (with respect to the fundamental component) with the phase angles of -25 and 35 degrees, respectively, which are considered to be fixed during simulations. Based on the data provided in Table 1, it can be seen that the value of impedance Z_{11} is considered to be twice that of impedance Z_{12} so that an asymmetric state is modeled for the MG. The reference values of the active powers of DG_1 and DG_2 are P^*_1=2000 W and P^*_2=1000W and the reference values of their reactive powers are Q^*_1=500 VAr and Q^*_2=250 VAr, respectively.

In order to investigate and analyze the performance of control systems of DGs in compensating for the voltage or current harmonics, the simulation is carried out in a continuous way and its results are presented in four separate periods.

- In the first period (0sec ≤ t < 2sec), only the virtual impedance of the fundamental component is active and no compensation is carried out.
- In the second period (2sec≤ t <3.5sec), the harmonic virtual impedance is activated but there is no compensation.
- In the third period (3.5sec≤ t <5sec), the PCC voltage harmonics compensation is activated.
- In the fourth period (3.5sec≤ t <5sec), the main grid current harmonics compensation is activated.

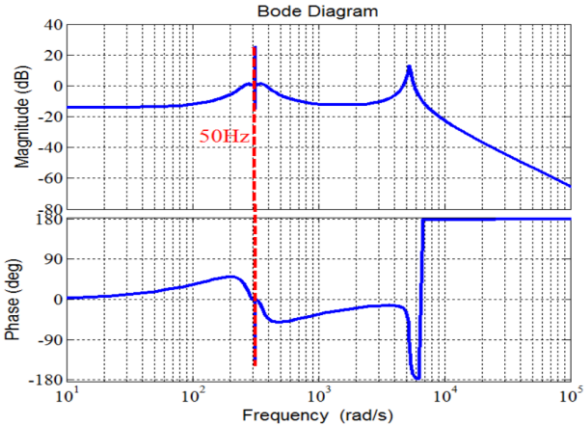

Fig. 8. Bode diagram of transfer function of closed loop control system.

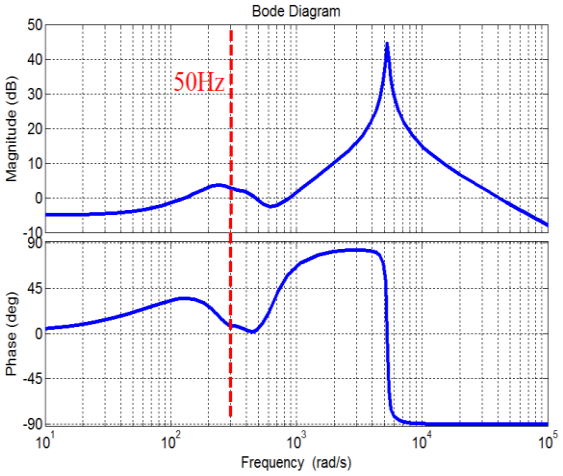

Fig. 9. Bode diagram of DG output impedance.

Table 1. Parameters of power stage of the electrical system used to compensate for voltage and current harmonics

Distribution line of DGs	Z_{l1}, Z_{l2} (Ω-mH)	0.15-1.5, 0.3-3
Distribution line of nonlinear load	Z (Ω-mH)	0.15-1.5
Distribution line+ network transformer	Z_g+Z_t(Ω-mH)	1-6
Linear load	Z_l (Ω-mH)	50-20
Nonlinear load	C_{NL}(μF), R_{NL}(Ω), L_{NL}(mH)	0.084, 100, 235

Table 2. Parameters of control system of DGs used to compensate for voltage and current harmonics.

Active and reactive power controllers		
DG_1 , DG_2	m_{pp}(rad/W)	10^{-6}, 2×10^{-6}
	m_{ip} (rad/W.s)	10^{-4}, 2×10^{-4}
	n_{pQ} (rad/W)	0.6×10^{-1}, 1.2×10^{-1}
	n_{iQ} (rad/W.s)	10^{-1}, 2×10^{-1}
Virtual impedance		
DG_1 , DG_2	R_V(mH)	0.1, 0.2
	L_V (mH)	2, 4
	K_v	0.004, 0.008
Voltage and current controllers	k_{pV}	0.25
	k_{pI}	0.35
	k_{rV}	12.5
	k_{rI}	250
	ω_{cV}/ω_{cI}(rad/s)	1
STF	ω(rad/s)	314
	k	30
Harmonic compensation	k_{Gv}	10
	k_{GI}	92

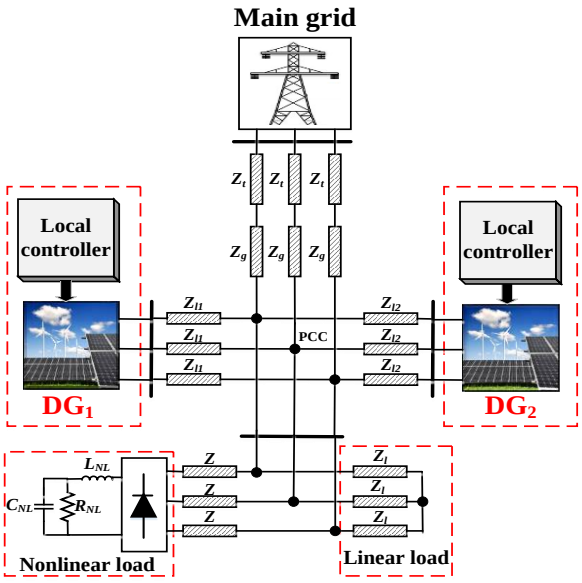

Fig. 10. Overall structure of grid-connected MG used for simulation.

- **First stage of simulation**

Fig. 11 shows three phase output voltages of DGs and PCC during the related period. As can be seen in this figure, before activating the harmonic virtual resistances, the output voltages of DGs are almost sinusoidal and without harmonics, which can be observed in Fig. 12 as small values of THD. In fact, the results of the first stage of simulation show that these voltage controllers have properly tracked the reference generated by the droop characteristics of the power controller. However, it can be seen that in spite of nearly sinusoidal output voltages of DGs, the PCC voltage is significantly distorted. Indeed, the main cause of this distortion is the harmonic voltage drop across distribution lines connecting DGs. The variations of the active and reactive powers of the fundamental component are shown in Figs. 13 (a) and (b). As can be seen, the references of the active and reactive powers are properly tracked. Fig. 14 shows that before adding harmonic virtual impedances at the first stage, S_n is shared between DGs in almost reverse proportion with their line impedance. This means that the amount of S_n supplied by DG_2 is almost twice of the amount supplied by DG_1 whereas the nominal power of DG_2 is half of the nominal power of DG_1. The output current of DGs and the three phase current of the main grid are shown in Fig. 15. As

can be observed, at the first stage, the total current supplied by DGs is not proportional to their nominal powers. It should be mentioned that according to Figs. 13 (a) and (b), the fundamental component of the load is distributed properly, but improper nonlinear load sharing has prevented the output current of DGs from being proportional to their nominal powers.

In Fig. 16, the harmonic disturbance indices of the DGs and the main grid output currents are shown. It can be seen that, at the first stage, the current harmonic disturbance of DG2 and the main grid have the maximum and minimum values, respectively. As discussed, at this stage, the existing impedances in the system determine the harmonic load sharing.

- **Second stage of simulation**

At the second stage of simulation, the harmonics virtual resistances are added to the basic control structure of DGs at t=2s. These resistances are placed on the way of harmonic currents to improve the nonlinear load sharing between DGs. In Fig. 14, it can be seen that once these resistances are added, the sharing of the nonlinear load between DGs is significantly improved but still it is not proportional to the nominal power of DGs. Similarly, it can be observed in Fig. 15 that the ratio of the amplitude of the output currents of DGs has considerably approached the ratio of their nominal powers. On the other hand, according to the results of Figs. 11 and 12 for the second period, adding virtual resistances at harmonic frequencies causes the output voltage of DGs to increase and consequently increases PCC voltage distortion. In Figs. 13 (a) and (b), it is shown that at the second stage, the powers of fundamental components are kept in the reference values, which represents the efficiency

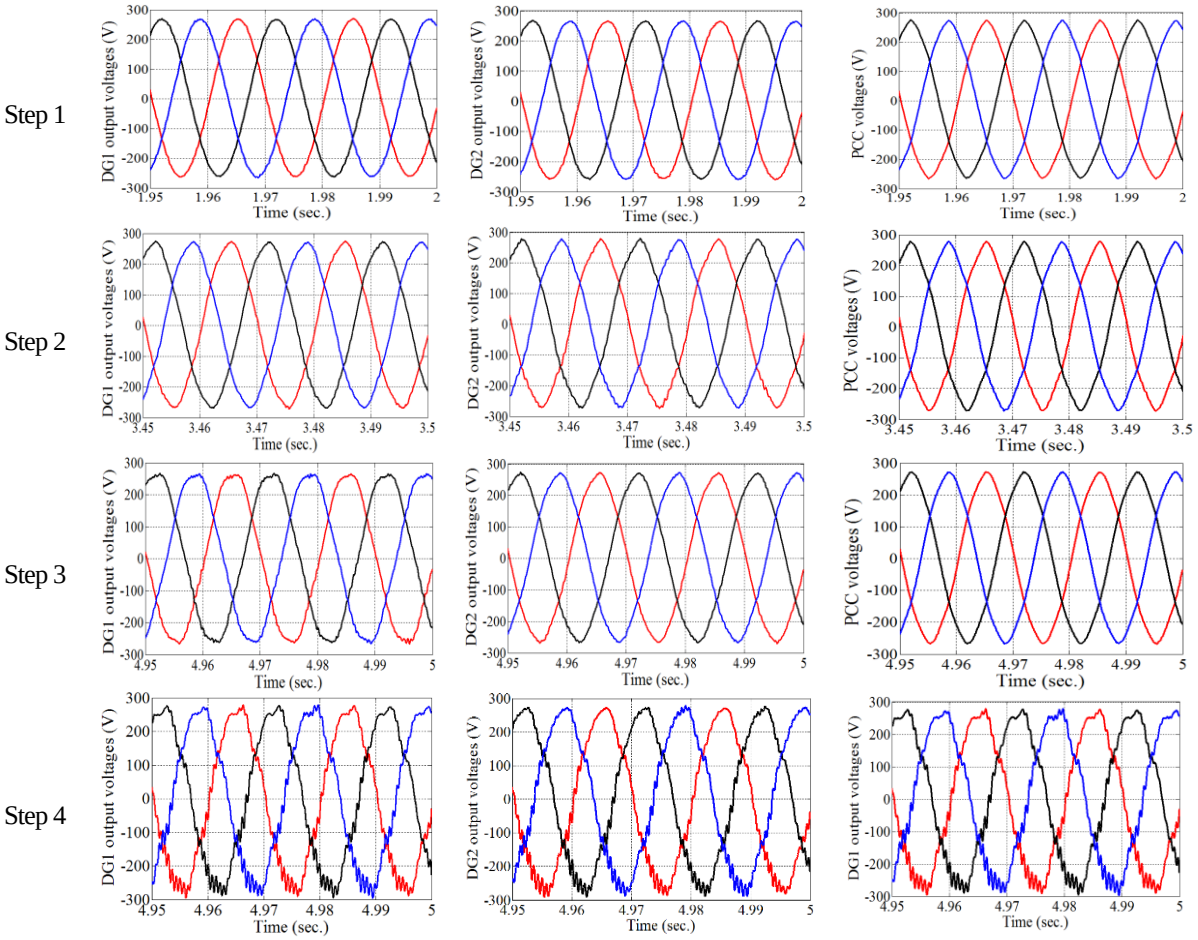

Fig. 11. Waveforms of three phase voltages at different simulation stages.

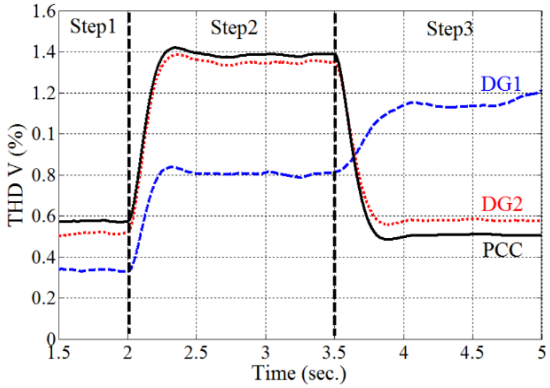

Fig. 12. Total harmonic distortion of voltage (fundamental component-100%).

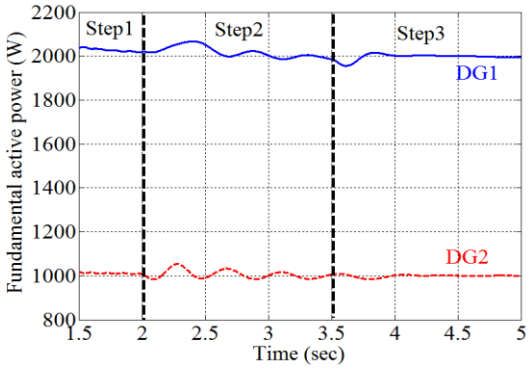

(a)

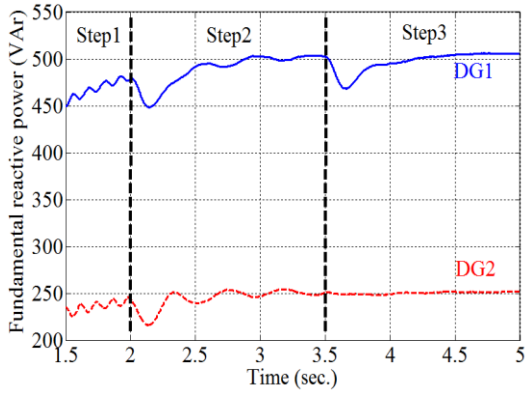

(b)

Fig. 13. Variations of the fundamental component: (a) active power (b) reactive power

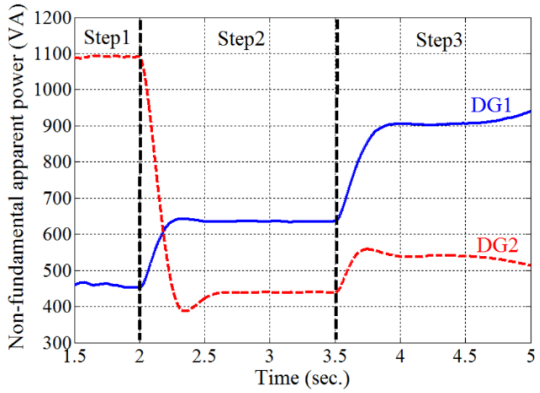

Fig. 14. Variation curves of non-fundamental apparent power.

- **Third stage of simulation**

In the third period, the voltage harmonics compensation units in local controllers of DGs are activated. It can be clearly seen in Fig. 12 that the voltage THD at PCC is significantly decreased. The improvement in the voltage quality at PCC can also be observed in Fig. 11. Also, it can be seen in Figs. 11 and 12 that voltage harmonics compensation is accompanied by an increase in DG_1 voltage distortion. In this regard, it must be noted that the impedance of the distribution line of the DG_1 is fairly greater than its corresponding value in DG_2, and considering its nominal power, the amount of the harmonic load supplied by this DG is greater than the one supplied by DG_2. Consequently, the voltage drop across the line of DG_1 and its harmonic virtual resistances cause a increase in PCC voltage distortion before compensation. After the compensation, the output voltage distortion of this DG is increased in order to provide an almost sinusoidal voltage at PCC after harmonic voltages across the distribution line and virtual resistances. On the other hand, due to the small values of the impedance of the distribution line of DG_2 and nonlinear load supplied by it, as observed in Figs. 11 and 12, the change in harmonic distortion of this DG as a result of the activation of compensation, is similar to PCC.

Furthermore, it is shown in Fig. 14 that during the compensation of PCC voltage harmonics, the powers of non-fundamental component of DG is increased. This increase is mainly because the current harmonics of DGs is increased so that compensation for the voltage harmonics becomes possible. Also, since the nominal power of the DG_1 is twice that of DG_2, it must have a greater share in compensation. Therefore, the results of the third stage of simulation show a greater increase in the power of non-fundamental component and harmonic distortion at the output voltage and current of DG_1 compared to DG_2.

It can be seen in Fig. 13 that the fundamental component powers also properly track their reference values at the third stage. On the other hand, it can be seen in Fig. 14 that after PCC voltage harmonics compensation, nonlinear load sharing between DGs is significantly improved and

this power is shared between DGs almost in proportion with their nominal powers. This improvement in nonlinear load sharing between DGs shows the efficiency of the proposed structure for harmonic virtual resistances and the efficiency of the solution selected for workload sharing.

- **Fourth step of simulation**

At this stage, the current harmonics compensation unit of the main grid is activated instead of the voltage harmonics compensation unit of PCC. As can be seen in Fig. 17, the THD of the main grid current is decreased. Also, it can be seen in this figure that the quality of the main grid current is improved with the increase in the disturbance of the DGs output current, which shows that these DGs supply a major part of harmonic current supplied by the main grid before compensation. This fact is shown by comparing the current waveforms of the fourth stage with those of the second stage. This comparison is shown in Fig. 15. The powers of the fundamental component also track the reference values properly. But the results are not shown since they are very similar to those presented in Fig. 13. Also, it is demonstrated in Figs. 15 and 18 that the load sharing in stage 4 is significantly increased in comparison with stage 2. The obtained results show the proper performance of the harmonic virtual impedances and the approach of sharing the compensation workload.

5. COMPARING RESULTS OF THE APPROACH PROPOSED IN [18]

In Ref. [18], an approach has been presented for for to compensate for voltage harmonics in islanded MGs. The block diagram of the control approach presented in Ref. [18] is shown in Fig. 19. In Fig. 19, H is referred to as the harminc power and is calculted as follows:

$$H = \sqrt{\tilde{p}_{rms}^2 + \tilde{q}_{rms}^2} \tag{17}$$

where $\tilde{p}_{rms}$ and $\tilde{q}_{rms}$ are the effective values of the oscillating parts of the active and reactive powers, respectively. H is the non-fundamental power (S_n) which is calculted in another way. In Fig. 19, the reference harmonic conduction (G^*) is determined based on G-H droop characteristics.

$$G^* = G_0 - b(H_0 - H) \tag{18}$$

where, b is a negative fixed value which needs to be set as the maximum possible value (from the point of view of absolute value, while keeping the control system stable), and it determines the slope of the drop characteristics. G_0 is a constant which, according to Ref. [18], can be considered as zero. H_0 is the rated harmonic reactive power. In Ref. [18], no specific method was presented for determining H_0. However, this parameter must be set in a way that $(H_0\text{-}H) > 0$ is satisfied. This droop charcteristics is considered for sharing the compensation workload between DGs.

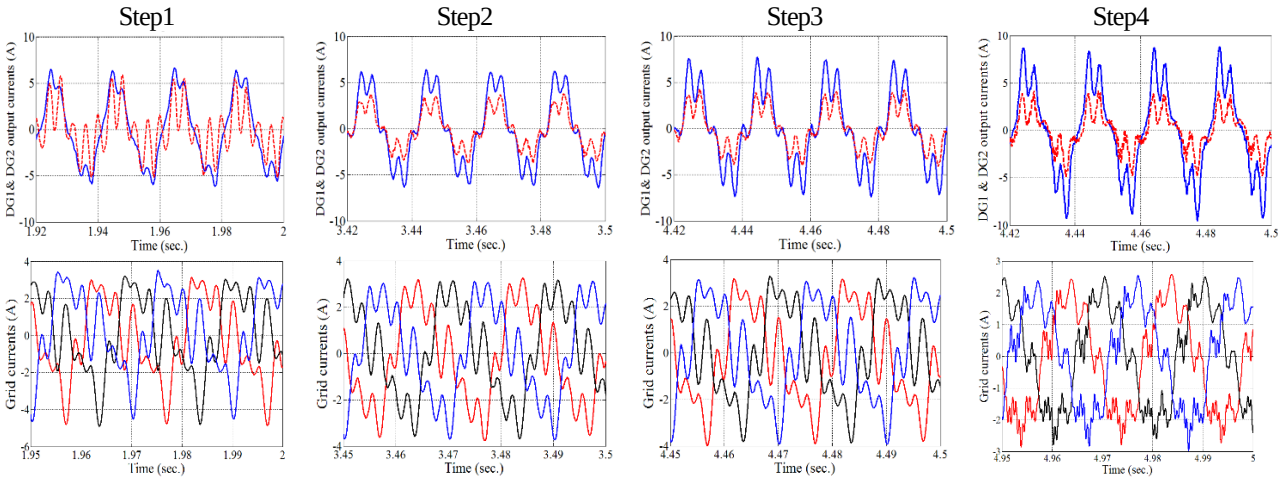

Fig. 15. Waveforms of three phase output current of DGs at different simulation stages.
The second line: the current of phase a (DG_1: Solid line, DG_2: Dashed line)

In this section, in order to reveal the advantages of the proposed approach, the results obtained by applying the method presented in Ref. [18] on the MG shown in Fig. 10 are presented and compared to those obatined using the proposed control approach. According to Ref. [18], b and H_0 need to be determined based on the rated capacity of DGs. Furthermore, for an MG consisting of two DGs (as shown in Fig. 10), the following eqaution has to be satisfied:

$$b_1.H_{01} = b_2.H_{02} \quad (19)$$

This equation means that the G-H characteristics of the DG with higher capacity must have a lower slope so that the compensation workload is shared properly. Thus, the following values are determined for the parameters:

$$b_1 = -0.0005, b_2 = -0.001, H_{01} = 2000, H_{02} = 1000$$

It should be noted that since the virtual harmonic resistances are not present in the approach used in [18], the second step of simulation (Section 4) is eliminated. The fourth step which is related to the compensation of current harmonics of the main network will also be eliminated. Therefore, only at t=3.5s harmonics compensation is activated (equivalent to the third step described in Section 4). Fig. 20 shows the results of sharing the fundamental and non-fundamental (H) powers. It is seen that the active and reactive powers are properly shared between DGs. But due to the absence of the harmonic virtual resistances, the non-fundamental power is not in proportion with the capacity of DGs. This shows the superiority of the approach presented in this paper (by comparing Figs. 14 and 20 (c)).

The THD of the ouput voltages of DGs and the load bus are shown in Fig. 21. It is seen that even in the absence of the harmonic virtual resistance, the output voltages of DGs are considerably distorted before compensation. Since controlling the voltage in the entire harmonic spectrum is performed by a PI controller, the harmonics of the output current are not controlled properly. However, in the voltage and current controllers proposed in this paper, a separate resonance expression is considered for harmonics as well as the fundamental component. Furthermore, it is seen that after activating the compensation of harmonics, the THD of output voltages of DGs is reduced to some extent. However, the disturbance of PCC voltage has a signinficant amount which can cause problems in operation of sensitive loads. But, considering Figs. 11 and 12, the proposed approach significantly improves the quality of the PCC voltage.

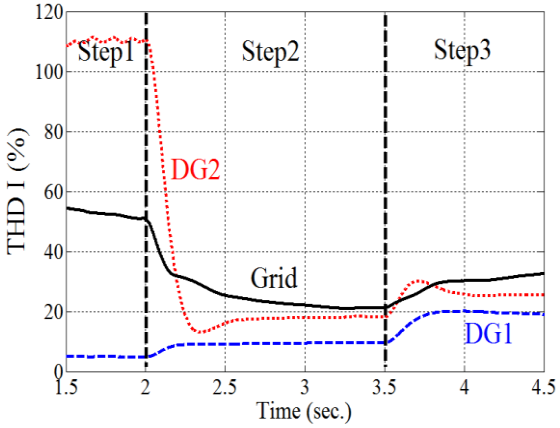

Fig. 16. Total harmonic distortion of current (fundamental component-100%).

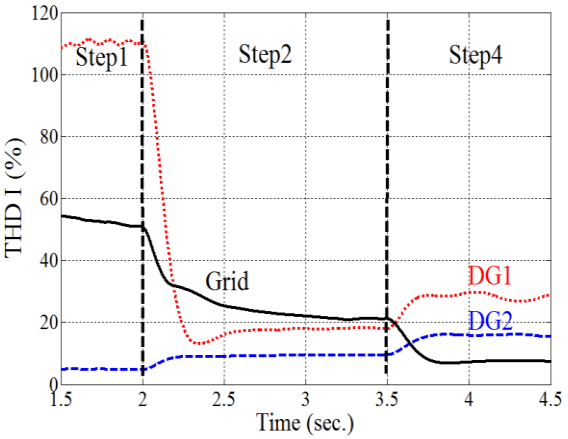

Fig. 17. Total harmonic distortion of current (fundamental component-100%).

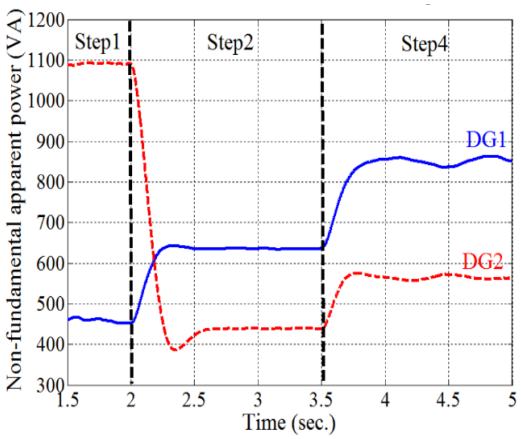

Fig. 18. Variation curves of non-fundamental apparent power.

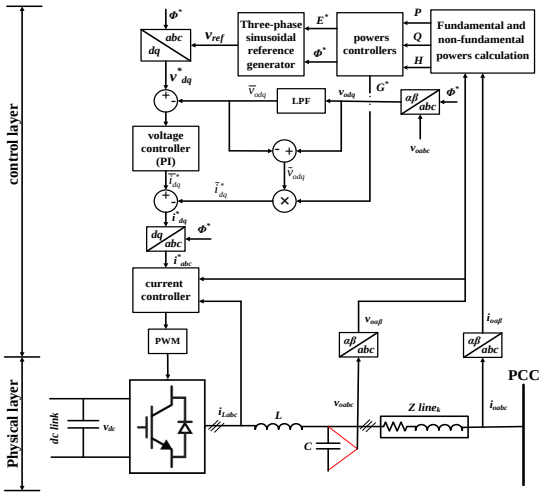

Fig. 19. The control system proposed in [18].

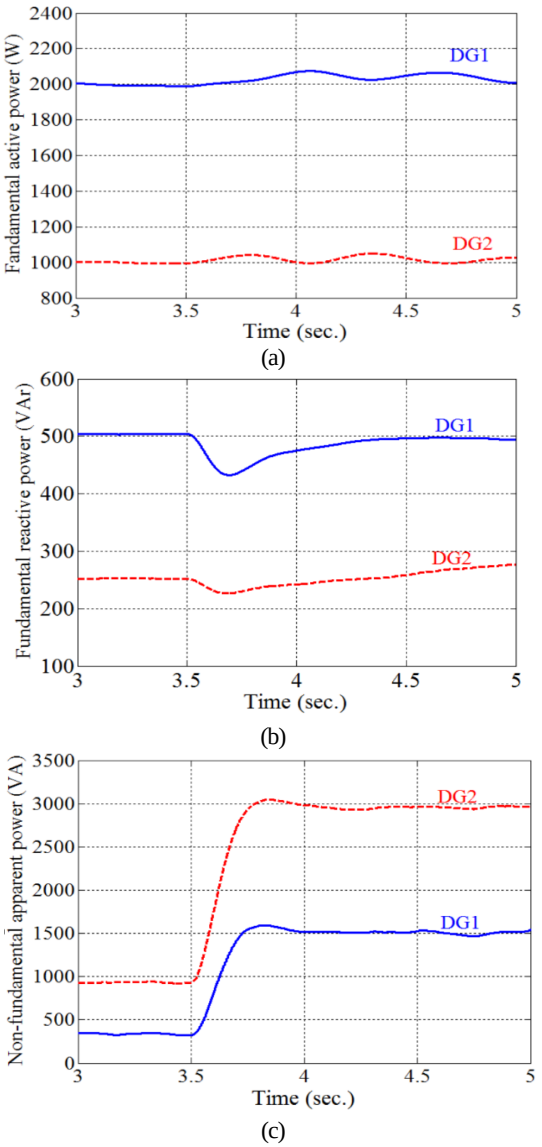

Fig. 20. (a) active power (b) reactive power (c) non-fundamental component power.

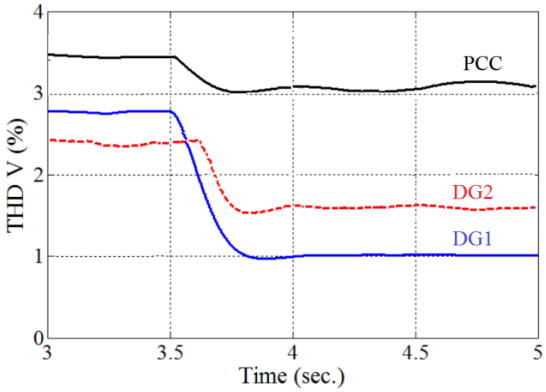

Fig. 21. Total harmonic distortion of DGs output voltage and PCC (fundamental component-100%).

6. CONCLUSION

In this paper, an approach was introduced for the compensation of voltage or current harmonics in grid-connected MGs, which could adjust compensation percentage in an adaptive way, in proportion with the existing amount of the distortion at the PCC or main grid. In this approach which was based on local control of DG units, harmonics compensation was performed in two scenarios. Both compensation scenarios were performed by DGs interface converters. Also, in local control of DG system, a structure was proposed for the virtual impedance which can share the fundamental and non-fundamental (nonlinear load) components among DGs in an adaptive way. The values of harmonic resistances were determined based on the amount of nonlinear load supplied by the DGs. Thus, the effect of asymmetry between the impedances of MGs was significantly decreased. The structure proposed for virtual impedance was capable of providing a proper nonlinear load sharing in MGs that are significantly asymmetric from lines impedance or load distribution points of view. The results showed that by using the proposed approach, the quality of PCC voltage and main grid current was remarkably improved, also the powers of fundamental and non-fundamental (nonlinear load) were shared in proportion between DGs.

REFERENCES

[1] IEEE Standard 1547.4-2011, "IEEE guide for design, operation, and integration of distributed resource island systems with electric power systems", 2011.

[2] M. Allahnoori, Sh. Kazemi, H. Abdi and R. Keyhani, "Reliability assessment of distribution systems in

presence of microgrids considering uncertainty in generation and load demand", *Journal of Operation and Automation in Power Engineering*, vol. 2, no. 2, pp. 113-120, 2014.

[3] S. Chowdhury, S.P. Chowdhury and P. Crossley, Microgrids and active distribution networks, Published by The Institution of Engineering and Technology (IET), London, United Kingdom, 2009.

[4] A. Mokari, H. Seyedi, B. Mohammadi-Ivatloo and S. Ghasemzadeh, "An improved under-frequency load shedding scheme in distribution networks with distributed generation", *Journal of Operation and Automation in Power Engineering*, vol. 2, no. 1, pp. 2-31, 2014.

[5] R. C. Dugan, M. F. McGranaghan, S. Santoso and H. W. Beaty, Electrical power systems quality, (2nded), New York: McGraw-Hill, 2003.

[6] A. Tuladhar, H. Jin, T. Unger and K. Mauch, "Parallel operation of single phase inverter modules with no control interconnections", in *Proceedings of the Twelfth annual Applied Power Electronics Conference and Exposition,* Atlanta, GA, pp. 94-100, 1997.

[7] J. M. Guerrero, J. Matas, L. G. de Vicuña, M. Castilla and J. Miret, "decentralized control for parallel operation of distributed generation inverters using resistive output impedance", *IEEE Transaction on Industrial Electronics*, vol. 54, no. 2, pp. 994-1004, 2007.

[8] P. Sreekumar and V. Khadkikar, "A new virtual harmonic impedance scheme for harmonic power sharing in an islanded microgrid", *IEEE Transaction on Power Delivery*, vol. 31, no. 3, pp. 936-945, 2015.

[9] M. Guerrero, J. Matas, L. G. Vicuna, M. Castilla and J. Miret, "Wireless control strategy for parallel operation of distributed generation inverters," *IEEE Transaction on Industrial Electronics*, vol. 53, no. 5, pp. 1461-1470, 2006.

[10] D. De and V. Ramanarayanan, "decentralized parallel operation of inverters sharing unbalanced and nonlinear loads", *IEEE Transaction on Power Electronics*, vol. 25, no. 12, pp. 3015-3025, 2010.

[11] M. Savaghebi, J.C. Vesquez, A. Jalilian, J.M. Guerrero and T. L. Lee, "Selective compensation of voltage harmonics in grid-connected microgrids," *International Journal of Mathematics and Computers in Simulation*,vol. 91, no. 6, pp. 211-228. 2013.

[12] M. Cirrincione, M. Pucci and G. Vitale, "A single-phase dg generation unit with shunt active power filter capability by adaptive neural filtering", *IEEE Transactions on Industrial Electronics*, vol. 55, no. 5, pp. 2093-2110, 2008.

[13] W. Al-Saedi, S. W. Lachowicz, D. Habibi and O. Bass, "Power quality enhancement in autonomous microgrid operation using particle swarm optimization," *International Journal of Electrical Power & Energy Systems*, vol. 42, no. 1, pp. 139-149, 2012.

[14] W. Al-Saedi, S. W. Lachowicz, D. Habibi and O. Bass, "Voltage and frequency regulation based DG unit in an autonomous microgrid operation using Particle Swarm Optimization," *International Journal of Electrical Power & Energy Systems*, vol. 53, no. 4, pp. 742-751, 2013.

[15] M. Prodanovic, K. D. Brabandere, J. V. Keybus, T. C. Green and J. Driesen, "Harmonic and reactive power compensation as ancillary services in inverter-based distributed generation", *IET Proceedings on Generation, Transmission and Distribution*, vol. 1, no. 3, pp. 432-438, 2007.

[16] J. He, Y. W. Li and M.S. Munir, "A flexible harmonic control approach through voltage controlled dg-grid interfacing converters", *IEEE Transaction on Industrial Electronics*, vol. 59, no. 1, pp. 444-455, 2012.

[17] X. Wang, F. Blaabjerg and Z. Chen, "Autonomous control of inverter-interfaced distributed generation units for harmonic current filtering and resonance damping in an islanded microgrid," *IEEE Transactions on Industry Applications*, vol. 50, no. 1, pp. 452-461, 2014.

[18] T.L. Lee and P.T. Cheng, "Design of new cooperative harmonic filtering strategy for distributed generation interface converters in an islanding network", *IEEE Transaction on Power Electronics*, vol. 22, no. 5, pp. 1919-1927, 2007.

[19] M. Savaghebi, J. M. Guerrero, A. Jalilian, J.C. Vasquez and Tzung-Lin Lee, "Hierarchical control scheme for voltage harmonics compensation in an islanded droop-controlled microgrid," *Proceedings of the IEEE Power Electronic and Drive Systems*, Singapore, pp. 89-94, 2011.

[20] M. M. Hashempour, M. Savaghebi, J.C. Vasquez and J. M. Guerrero, "A control architecture to coordinate distributed generators and active power filters coexisting in a microgrid", *IEEE Transaction on Smart Grid*, vol. PP, no. 99, pp. 1-12, 2015.

[21] S. Anwar , A. Elrayyah and Y. Sozer, "Efficient single phase harmonics elimination method for microgrid operations", *IEEE Transaction on Industry Applications*, vol. 51, no. 4, pp. 3394-3403, 2015.

[22] J.M. Guerrero, M. Chandorkar, T.L. Lee and P.C.

Loh, "Advanced control architectures for intelligent microgrids - part ii: power quality, energy storage, and ac/dc microgrids," *IEEE Transaction on Industrial Electronics*, vol. 60, no. 4, pp. 1263-1270, 2013.

[23] H. Akagi, E.H. Watanabe and M. Aredes, Instantaneous power theory and applications to power conditioning, Wiley-IEEE Press, 2007.

[24] J.M. Guerrero, J.C. Vasquez, J. Matas, L.G. de Vicuna and M. Castilla, "Hierarchical control of droop-controlled ac and dc microgrids - a general approach toward standardization", *IEEE Transactions on Industrial Electronics*, vol. 58, no. 1, pp. 158-172, 2011.

[25] F. Blaabjerg, R. Teodorescu, M. Liserre and A.V. Timbus, "Overview of control and grid sync hronization for distributed power generation systems", *IEEE Transactions on Industrial Electronics*, vol. 53, no. 5, pp. 1398-1409, 2006.

[26] P.C. Loh and D.G. Holmes, "Analysis of multiloop control strategies for lc/cl/lcl filtered voltage sourse and current source inverters", *IEEE Transactions on Industrial Applications*, vol. 41, no. 2, pp. 644-654, 2005.

[27] H. Song, H. Park and K. Nam, "An instantaneous phase angle detection algorithm under unbalanced line voltage condition," in *Proceedings of the* 30*th Annual IEEE Power Electronics Specialists Conference*, Charleston, SC, pp. 533-537, 1999.

[28] M. Abdusalam, P. Poure, S. Karimi and S. Saadate, "New digital reference current generation for shunt active power filter under distorted voltage conditions", *Electric Power Systems Research*, vol. 79, no. 2, pp. 759-765, 2009.

[29] R. Ghanizadeh and M. Ebadian, "Improving the performance of UPQC under unbalanced and distortional load conditions: A new control method", *Journal of Artificial Intelligence & Data Mining*, vol. 3, no. 2, pp. 225-234, 2015.

[30] M. Ebadian, M. Talebi and R. Ghanizadeh, "A new approach based on instantaneous power theory for improving the performance of UPQC under unbalanced and distortional load conditions", *Automatika - Journal for Control, Measurement, Electronics, Computing and Communications*, vol. 56, no. 2, pp. 52-64, 2015.

[31] J. He and Y. W. Le, "Analysis and design of interfacing inverter output virtual impedance in a low voltage microgrid," *Proceedings of the IEEE Energy Conversion Congress and Exposition*, Atlanta, GA, pp. 2847-2864, 2010.

[32] IEEE Standard 1459-2010, IEEE standard definitions for the measurement of electric power quantities under sinusoidal, no sinusoidal, balanced or unbalanced conditions, 2010.